Experimental Section

Lipid solution preparation. 1,2-dipalmitoyl-sn-glycero-3 phosphoglycerol (DPPG) was purchased in powder form Avanti Polar Lipids, Inc.; lipid A (diphosphoryl from Escherichia coli F583) was purchased in powder from Sigma-Aldrich. Solution of DPPG was prepared in chloroform:methanol 2:1 (v/v) (HPLC grade, Sigma-Aldrich) and of lipid A in chloroform:methanol:water 74:23:3 (v/v).

Antimicrobial agent preparation. AA-1 was prepared as in our previous publication [1]. The OAK was synthesized by the solid-phase method applying the Fmoc active ester chemistry [2] as described [3]. The crude OAK was purified to chromatographic homogeneity (>95% purity) by reverse-phase high-performance liquid chromatography (rpHPLC) and subjected to mass spectrometer analysis (Alliance-ZQ Waters). HPLC runs were performed on C18 columns (Vydac) using a linear gradient of acetonitrile in water (1%/minute), with both solvents containing 0.1% TFA. The purified OAK was stocked as lyophilized powder at −20 °C. Prior to being tested, fresh solutions were prepared in water (mQ; Millipore), vortexed, sonicated, centrifuged, and then diluted in the appropriate medium.

Langmuir surface balance. Surface pressure-molecular area (π-A) measurements and insertion assays were performed using a custom-built thermostatted twin-barrier Teflon Langmuir trough mounted onto a vibration isolation stage (Newport Corporation, Irvine, Ca) and equipped with a Wilhelmy plate surface tension measuring system (Riegler & Kirstein, Potsdam, Germany). A series of thermoelectric heating elements (Omega Engineering, Inc.) placed just beneath the trough and accompanied by a feedback control enabled us to set the temperature with 0.2 °C precision. In order to reduce evaporation, contamination, and convection effects a resistively heated indium tin oxide-coated glass plate (Delta Technologies, LTD) was placed over the trough. The setup was controlled by in-house software developed in LabView 7.1 (National Instruments). The experiments were carried out on Dulbecco's phosphate buffered saline without calcium and magnesium (D-PBS) (Invitrogen) at 23 ± 0.2 °C.

Insertion assays. Constant-pressure insertion experiments were carried out to quantify the interactions of peptidomimetic compounds with membrane mimics. Monolayers were formed by depositing the droplets of respective solution at the air-liquid interface up to the surface coverage of 75%. After equilibrated for 15 minutes, the monolayers were compressed to the surface pressure of 30 mN/m, which is equivalent to the packing density of the cell membrane [4]. The surface pressure was kept constant via proportional-integral-derivative feedback control. The solution of respective peptidomimetic compound was then evenly injected underneath the monolayers using a micro-syringe with an L-shaped needle (Hamilton, Reno, NV) to make up the final concentration of 1.3 μM for OAK-1 and of 9 μM for AA-1. Injected compounds interact with the lipid monolayers and result in an increase in the surface pressure when incorporate into the membrane. To keep the surface pressure constant, the surface area would have to increase. The resulting relative change in area per molecule, ΔA/A, was monitored for up to 40 minutes after insertion.

XR and GIXD. Liquid surface X-ray scattering experiments were performed at the Chemistry and Materials Section of the Consortium for Advanced Radiation Sources (ChemMat-CARS) beamline of the Advanced Photon Source at Argonne National Laboratory [5]. Both XR and GIXD are well-established techniques for studying Langmuir films [6]. GIXD was employed to investigate an impact of OAK-1 and AA-1 on an in-plane molecular order of bacterial membrane mimics. Depth of antimicrobials' insertion was determined using XR. The wavelength of the beam was set to $\lambda = 1.23744$ Å. XR data were analyzed using model-dependent "slab" model refinement [4a-c] and model-independent stochastic fitting [7] routines employing RFIT2000 (Oleg Konovalov, ESRF) and Stochfit software [7].

Analysis of x-ray reflectivity data on incorporation of AMP mimics into the model monolayers

Analysis of XR data allows us to determine the relative vertical position of OAK-1 and AA-1 within the lipid monolayers. The X-ray reflectivity results, R(q), of the monolayer films before and after introduction of OAK-1 and AA-1 as a function of the normal momentum transfer q_Z, normalized by the Fresnel reflectivity $R_F(q_Z)$, is shown in Figure 1b,c. Electron density profiles ρ(z) were obtained by fitting the measured reflectivities using the model-dependent slab model refinement [4a, 4c, 8] as well as the model-independent stochastic fitting [7] routines. Both approaches resulted in very similar fits that are in excellent agreement with the measured reflectivity curves (Figure 1b,c). For convenience, the electron density profiles are discussed within the framework of the slab model hereafter. Table 1 summarizes the fitting results of the slab model refinement, including slab thickness (L), average electron density (ρ), and roughness (σ).

XR analysis of pure DPPG and lipid A monolayers required two slabs with the top slab composed of the acyl chains sticking into the air comprising thickness 16.9 Å for the DPPG and 15.2 Å for the lipid A and the corresponding electron density ρ being 0.318 $e^-/Å^3$ and 0.317 $e^-/Å^3$, respectively. The bottom slab is composed of lipid headgroups and is 8.1 Å thick with ρ of 0.504 $e^-/Å^3$ for the DPPG and 6.2 Å thick with ρ of 0.554 $e^-/Å^3$ for the lipid A. The XR results agree well with our earlier studies of DPPG [4a, 4c, 9] and lipid A [4b, 4c].

Introduction of OAK-1 and, especially, AA-1 underneath the monolayer films leads to profound changes in the reflectivity profiles of the anionic lipid monolayers (Figure 1b,c). Both compounds induce a shift in the position of the first minimum in the DPPG and lipid A reflectivity curves towards greater momentum transfer q_Z values, which, in case of OAK-1, is an indicative of decrease in the overall film thickness. However, the reflectivity data curves from the anionic lipid monolayers with AA-1 display an additional feature, a weak minimum at $q_Z \sim 0.47$ $Å^{-1}$, which points to the presence of film regions with increased thickness.

XR data of the anionic lipid monolayers with OAK-1 were fitted using three slab models (Table 1). The results of XR refinement together with the AMP compound insertion induced increase in molecular areas, suggest that the top slab for the anionic lipid/OAK-1 systems contains the upper portion of the lipid acyl chains, while the next slab includes the remainder of the lipid acyl chains and the backbone of the OAK-1 compound, and the slab next to the aqueous buffer consists of the lipid headgroups and the OAK-1 lysine chains (Figure 1).

Previous coarse-grain molecular dynamics simulations have suggested that arylamides such as AA-1 are likely to have two modes of binding to bilayers [10]. Indeed, the reflectivity of the DPPG monolayer upon AA-1 insertion (Table 1) was consistent with this expectation, requiring a complex model to account for the XR data. The model for the DPPG/AA-1 system contains five slabs. A likely assignment of the first three slabs from the top to the bottom are (a) the upper portion of the DPPG acyl chains, (b) the remainder of the DPPG acyl chains and the hydrophobic portion of inserted AA-1, including its t-butyl and phenyl units, (c) the DPPG headgroups and the hydrophilic part of AA-1. An additional two "lower" slabs, (d) and (e), are required to account for the entire density profile. These features are assigned to absorbed

AA-1 molecules (and perturbed, non-bulk water molecules), which form a second layer that beneath the "top" phospholipid/AA-1 monolayer. The overall molecular dimensions and electron density of slabs (d) and (e) suggest that they might be formed by a monolayer of the AA-1 molecules packed with their long axes parallel to the membrane normal or a bilayer of AA-1 with the axis of the individual molecules packed along the membrane surface.

The best fit to the reflectivity data for the lipid A/AA-1 system was achieved with a three slab model. A likely assignment of the slabs from the top to the bottom are (a) the lipid A acyl chains; (b) the lipid A headgroups and a part of AA-1; (c) the remaining part of AA-1 molecules (Figure 1). Figure 1 shows schematic cartoons of the proposed modes of insertion of OAK-1 and AA-1 into anionic lipid monolayers.

Table 1. X-ray reflectivity data fitting parameters for the DPPG and lipid A monolayers before and after injection of the antimicrobials.

Experiment	Description	L_i, Å	ρ_i, $e^-/Å^3$	σ, Å	ΔA/A, %
DPPG	AC[a]	16.9	0.318	3.6	-
	HG[b]	8.1	0.504		
lipid A	AC	15.2	0.317	3.3±0.2	-
	HG	6.2	0.554		
DPPG/OAK-1	AC	6.3	0.272		
	AC/OAK-1	8.4	0.352	3.5±0.2	38±2
	HG/OAK-1	8.9	0.427		
lipid A/OAK-1	AC	8.1	0.254		
	AC/OAK-1	6.7	0.357	3.7±0.2	38±2
	HG/OAK-1	5.4	0.396		
DPPG/AA-1	AC	8.9	0.217		
	AC/AA-1	9.3	0.471		
	HG/AA-1	7.8	0.388	3.7±0.6	60±4
	AA-1	14.3	0.361		
lipid A/AA-1	AA-1	9.9	0.351		
	AC	9.9	0.268		
	HG/AA-1	10.2	0.439	3.9±0.2	60±4
	AA-1	4.5	0.366		

[a]AC – lipid acyl chain region; [b]HG – lipid headgroup region.

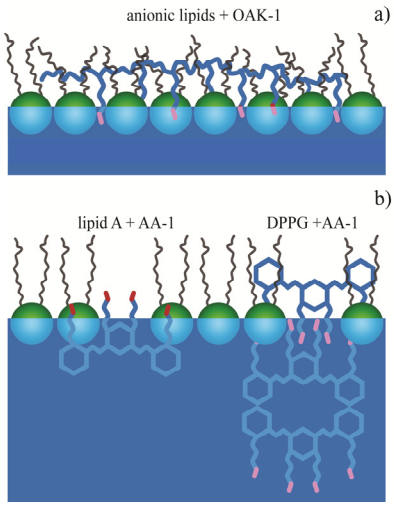

Figure 1. The cartoon-schematics of OAK-1 and AA-1 out-of-plane arrangement in the anionic lipid monolayers corresponding to the XR data analysis.

[1] S. Choi, A. Isaacs, D. Clements, D. H. Liu, H. Kim, R. W. Scott, J. D. Winkler, W. F. DeGrado, *Proc Natl Acad Sci USA* **2009**, *106*, 6968.
[2] G. B. Fields, R. L. Noble, *Int J Pept Protein Res* **1990**, *35*, 161.
[3] I. S. Radzishevsky, T. Kovachi, Y. Porat, L. Ziserman, F. Zaknoon, D. Danino, A. Mor, *Chem & Biol* **2008**, *15*, 354.
[4] a)F. Neville, M. Cahuzac, O. Konovalov, Y. Ishitsuka, K. Y. C. Lee, I. Kuzmenko, G. M. Kale, D. Gidalevitz, *Biophys J* **2006**, *90*, 1275; b)F. Neville, C. S. Hodges, C. Liu, O. Konovalov, D. Gidalevitz, *Biochim Biophys Acta Biomembr* **2006**, *1758*, 232; c)F. Neville, Y. Ishitsuka, C. S. Hodges, O. Konovalov, A. J. Waring, R. Lehrer, K. Y. C. Lee, D. Gidalevitz, *Soft Matter* **2008**, *4*, 1665; d)F. Neville, A. Ivankin, O. Konovalov, D. Gidalevitz, *Biochim Biophys Acta Biomembr* **2009**.
[5] B. H. Lin, M. Meron, J. Gebhardt, T. Graber, M. L. Schlossman, P. J. Viccaro, in *7th Int Conf Surface X-Ray Neutron Scatt*, Lake Tahoe, California, **2002**, pp. 75.
[6] J. Als-Nielsen, D. Jacquemain, K. Kjaer, F. Leveiller, M. Lahav, L. Leiserowitz, *Phys Rep* **1994**, *246*, 252.
[7] S. M. Danauskas, D. X. Li, M. Meron, B. H. Lin, K. Y. C. Lee, *J Appl Cryst* **2008**, *41*, 1187.
[8] F. Neville, A. Ivankin, O. Konovalov, D. Gidalevitz, *Biochim Biophys Acta Biomembr* **2010**, *1798*, 851.
[9] D. Gidalevitz, Y. J. Ishitsuka, A. S. Muresan, O. Konovalov, A. J. Waring, R. I. Lehrer, K. Y. C. Lee, *Proc Natl Acad Sci USA* **2003**, *100*, 6302.
[10] C. F. Lopez, S. O. Nielsen, G. Srinivas, W. F. DeGrado, M. L. Klein, *J Chem Theory Comput* **2006**, *2*, 649.